Conformational Changes during Normal and Error-Prone Incorporation of Nucleotides by a Y-Family DNA Polymerase Detected by 2-Aminopurine Fluorescence†

Angela M. DeLucia, Nigel D. F. Grindley, and Catherine M. Joyce*

Department of Molecular Biophysics and Biochemistry, Yale University, New Haven, Connecticut 06520

Received April 10, 2007; Revised Manuscript Received July 2, 2007

ABSTRACT: Y-family polymerases are specialized to carry out DNA synthesis past sites of DNA damage. Their active sites make fewer contacts to their substrates, consistent with the remarkably low fidelity of these DNA polymerases when copying undamaged DNA. We have used DNA containing the fluorescent reporter 2-aminopurine (2-AP) to study the reaction pathway of the Y-family polymerase Dbh. We detected 3 rapid noncovalent steps between binding of a correctly paired dNTP and the rate-limiting step for dNTP incorporation. These early steps resemble those seen with high-fidelity DNA polymerases, such as Klenow fragment, and include a step that may be related to the unstacking of the 5′ neighbor of the templating base that is seen in polymerase ternary complex crystal structures. A significant difference between Dbh and high-fidelity polymerases is that Dbh generates no fluorescence changes subsequent to dNTP binding if the primer lacks a 3′OH, suggesting that the looser active site of Y-family polymerases may enforce reliance on the correct substrate structure in order to assemble the catalytic center. Dbh, like other bypass polymerases of the DinB subgroup, generates single-base deletion errors at an extremely high frequency by skipping over a template base that is part of a repetitive sequence. Using 2-AP as a reporter to study the base-skipping process, we determined that Dbh uses a mechanism in which the templating base slips back to pair with the primer terminus while the base that was originally paired with the primer terminus becomes unpaired.

Y-family polymerases have low fidelity during synthesis on undamaged DNA and can bypass DNA lesions that normally block replication by high-fidelity polymerases (*1*). While these lesion-bypass polymerases share the common "right-hand" arrangement of the fingers, palm, and thumb subdomains conserved throughout the polymerase superfamily, they also have unique structural features that allow their active sites to accommodate mismatched or damaged bases (*2*−*13*). Unlike high-fidelity polymerases, Y-family polymerases have minimal protein interactions with their DNA and dNTP[1] substrates and therefore do not form a snug binding pocket surrounding the nascent base pair. Additionally, Y-family polymerases have a novel "little-finger" domain which functions in DNA binding and may also help determine their lesion bypass specificity (*2*, *4*−*7*, *14*, *15*).

Structures of high-fidelity polymerases show a conformational change within the fingers subdomain that results in an "open" to "closed" transformation of the active site when the Pol−DNA binary complex binds a correct dNTP, forming the Pol−DNA−dNTP ternary complex (*16*−*20*). This noncovalent step is believed to enhance polymerase fidelity by an "induced-fit" mechanism, in which the geometry of a correct nascent base pair favors progression along the reaction pathway toward phosphoryl transfer (*16*, *19*, *21*−*24*). By contrast, structural comparisons of apoenzyme, binary and ternary complexes from bypass polymerases imply that the fingers subdomain is permanently in a conformation equivalent to the closed conformation of high fidelity DNA polymerases. This has led to the suggestion that the active site is "preformed" even in the absence of DNA or dNTP (*2*−*4*, *7*, *10*). Comparison of binary and ternary complex structures of the Y-family polymerase Dpo4 reveals a different noncovalent change associated with dNTP binding (*15*). Unlike binary complexes in other polymerase families, the terminal base pair in the Dpo4 binary complex (2AU0) is in the expected location of the nascent base pair (*15*). Before chemistry, the contacts between the little-finger domain and the DNA slide by one nucleotide step so that the active site is available for binding the nascent base pair. This conformational change is entirely distinct from that seen in high-fidelity polymerases such as those from the A-family, where ternary complex formation does not require the DNA to translocate, and a rotation of the O-helix within the fingers subdomain forms a snug, solvent-excluded nascent base pair binding pocket prior to phosphoryl transfer (*16*, *19*, *25*).

Given the differences in fidelity and structures of Y-family and high-fidelity DNA polymerases, we are interested in how

† This work was supported by NIH Grant GM-28550.

* Send correspondence to this author: Department of Molecular Biophysics and Biochemistry, Yale University, Bass Center for Molecular and Structural Biology, 266 Whitney Avenue; P.O. Box 208114, New Haven, CT 06520-8114. Phone: (203) 432-8992 Fax: (203) 432-3104. E-mail: catherine.joyce@yale.edu.

[1] Abbreviations: dNTP, deoxynucleoside triphosphate; 2-AP, 2-aminopurine; Dbh, DinB homologue of *Sulfolobus acidocaldarius*; Dpo4, DNA polymerase IV of *Sulfolobus solfataricus*; Pol IV, *E. coli* DNA polymerase IV (DinB); Pol I (KF), Klenow fragment of *E. coli* DNA polymerase I; pol, (DNA) polymerase.

10.1021/bi7006756 CCC: $37.00
Published on Web 08/29/2007

Scheme 1[a]

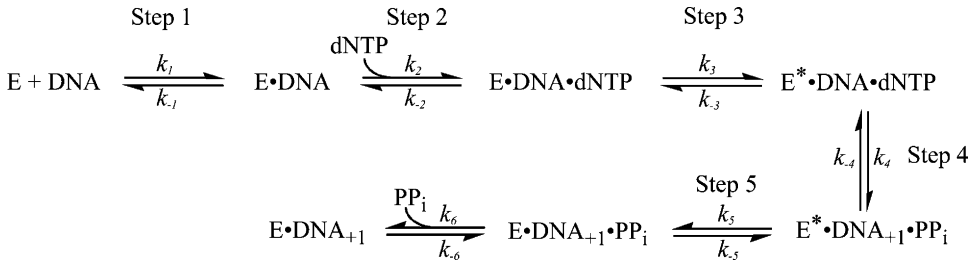

[a] Reprinted with permission from ref *39*. Copyright 2003 American Chemical Society.

their reaction pathways compare. Our model system is the Dbh (DinB homologue) polymerase from the thermophilic archaebacterium *Sulfolobus acidocaldarius*, a member of the DinB branch of the Y-family. Previous work by us and others has established the basic kinetic properties of Dbh and explored its specificity and error-prone behavior (*26*−*30*). Several apoenzyme structures of Dbh have been solved (*3*, *6*), and the structures of complexes with bound substrates can be inferred using cocrystal data from the close homologue, Dpo4, from *Sulfolobus solfataricus (2*, *10*, *15*). The amino acid sequences of Dbh and Dpo4 are 54% identical overall and 59% identical within the catalytic core (*14*). Domain-swap experiments imply that any mechanistic differences between these two polymerases are probably attributable to the little-finger domain and the linker region which tethers the little-finger domain to the thumb, where the homology between Dbh and Dpo4 is lowest (*14*).

Two Y-family polymerases, Dpo4 and eukaryotic DNA pol *η*, have been studied extensively by single-turnover kinetics using rapid chemical quench methods (*31*, *32*). In both cases, the minimal reaction pathway derived from these experiments resembles that of high-fidelity DNA polymerases such as Klenow fragment (Pol I (KF)) and T7 DNA pol, where the ordered binding of DNA and dNTP is followed by a rate-limiting noncovalent change (step 3) preceding phosphoryl transfer (*33*, *34*) (Scheme 1). The phosphoryl transfer step is fast and followed by a slow protein conformational change and release of pyrophosphate. DNA release from the binary complex is slow and most likely rate-limiting after the first turnover.

In our current study, we have used DNA labeled with the fluorescent reporter 2-aminopurine (2-AP) to identify early noncovalent changes that accompany ternary complex formation and correct dNTP insertion by Dbh. The use of fluorescence to detect noncovalent steps that are not accessible by chemical quench experiments has been very informative in studies of the reaction pathways of several high-fidelity DNA polymerases (*35*−*42*). 2-AP is a fluorescent adenosine analogue which forms a correct base pair with thymine and does not distort the DNA helix (*43*). The fluorescence of 2-AP is sensitive to changes in stacking with adjacent template bases or protein side chains and can therefore report on the immediate environment of the substituted base (*44*).

Our fluorescence study of the Dbh reaction pathway includes a reaction that is characteristic of Dbh, Dpo4, *E. coli* Pol IV (DinB), and other members of the DinB subgroup of the Y-family. These DNA polymerases have particularly high error rates for deletion mutations at a characteristic template sequence, consisting of a homonucleotide run of 2 or more bases with an immediately adjacent 5′G (*26*, *45*, *46*). During DNA synthesis, one of the repeated template bases is skipped over, resulting in a single-base deletion error. We have used the 2-AP fluorescent reporter to investigate how the template strand DNA is accommodated at the active site when a template base is skipped.

FIGURE 1: Sequence of DNA substrates used in this study. For each DNA sequence 2-AP substitution is indicated by an X. Our numbering of the positions within the template strand is indicated on substrate I.

EXPERIMENTAL PROCEDURES

Materials. Purification of wild-type Dbh followed our previously published procedures (*26*, *27*). Synthesis of DNA oligonucleotides was carried out by the W. M. Keck Biotechnology Resource Laboratory at Yale Medical School. Annealed primer/template DNA substrates for chemical quench and stopped-flow reactions were prepared as previously described (*26*). The DNA sequences used in this study are shown in Figure 1. Ultrapure dNTPs were purchased from Amersham Pharmacia Biotech. dTMP was purchased from Sigma-Aldrich.

Chemical Quench Measurements. All kinetic measurements were carried out at 22 °C under single-turnover conditions, based on our published methods (*26*, *27*) with the following modifications. Reactions were initiated by mixing equal volumes of a dNTP and a Dbh−DNA solution. The dNTP solution contained extra $MgCl_2$, equimolar with the dNTP concentration, in addition to the 10 mM $MgCl_2$ already present in the Dbh reaction buffer. A typical reaction contained final concentrations of 100 nM annealed primer/template DNA, 2.5 μM Dbh, 5 mM DTT, 50 mM Hepes (pH 8.5), 10 mM $MgCl_2$, and varied dNTP/$MgCl_2$ concentrations. A rapid quench−flow apparatus (KinTek Corp., Model RQF-3) was used for reactions that were too fast for manual quenching.

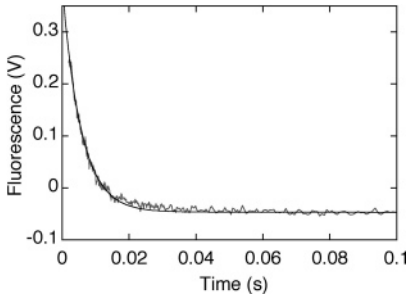

FIGURE 2: Dissociation of DNA substrate I from the Dbh−DNA binary complex measured by stopped-flow fluorescence. The solid line shows the best fit of the data to a single exponential followed by a linear phase, giving a DNA dissociation rate of 180 s^{-1} and a photobleaching rate of 0.002 s^{-1}.

Stopped-Flow Fluorescence and Analysis. Stopped-flow experiments were performed at 22 °C using an Applied Photophysics SX.18MV spectrofluorometer. To measure dNTP incorporation by Dbh, one drive syringe contained Dbh bound to a 2-AP DNA substrate and the other contained dNTP/$MgCl_2$, as described above. Rapid mixing of these two solutions gave final concentrations of 200 nM DNA, 3 μM Dbh, 5 mM DTT, 50 mM Hepes (pH 8.5), 10 mM $MgCl_2$, and varied concentrations of dNTP/$MgCl_2$ (0.5−12 mM), as indicated in each figure. DNA dissociation from the Dbh−DNA binary complex was measured by mixing a solution of 260 nM Dbh and 400 nM of the 2-AP DNA substrate with a solution containing a 20-fold excess of unmodified primer/template DNA. The excitation wavelength used for 2-AP was 313 nm, and fluorescence emission was detected with a 345 nm long-pass filter. Individual traces were acquired for at least 10 s using a logarithmic timebase, and an average from at least 3 traces was taken for each dNTP concentration. Fluorescence traces were fitted to a double or triple exponential equation using Kaleidagraph (Synergy Software, Reading, PA).

Fluorescence Emission Spectra. Steady-state fluorescence spectra were recorded at 22 °C using a Photon Technology International scanning spectrofluorometer. Samples of 2-AP DNA (10 μM DNA, 10 mM $MgCl_2$, 50 mM Hepes (pH 8.5)) were excited at 310 nm, and emission spectra were collected from 320 to 460 nm. Emission spectra of Dbh−DNA complexes were measured using solutions containing 1 μM DNA, 5 μM Dbh, 10 mM $MgCl_2$, 5 mM DTT, 50 mM Hepes (pH 8.5), and, as required, 4 mM dNTP (indicated in Figure 5C). All emission spectra were corrected by subtraction of emission data from identical control solutions lacking the 2-AP-containing DNA.

RESULTS

2-AP-Containing DNA Substrates. We used 2-AP as a fluorescent reporter for identifying noncovalent changes during nucleotide binding and incorporation by Dbh. Figure 1 shows the sequences of the 2-AP-containing DNA substrates (I−IV) used in this study. Based on studies in other systems which have been informative about conformational transitions during the polymerase reaction (*35*−*42*), we positioned 2-AP either as the first unpaired base within the template overhang (designated as the templating base or 0 position) or as the base immediately 5′ to this position (designated as the +1 template base). To study the base-skipping reaction, we used 2-AP as the template base of the terminal base pair (designated as the −1 position). The majority of our experiments were carried out with a 3′OH-containing primer, so as to allow primer extension to occur. In some experiments we used a 2′,3′-dideoxy-terminated primer to block catalysis, based on studies in other polymerase systems where this strategy has facilitated detection of precatalytic conformational changes (*36*, *39*, *41*, *42*). Because of the weak dNTP binding by Dbh (*26*, *28*), it was necessary to use very high concentrations of dNTP/$MgCl_2$ (up to 12 mM final) in order to examine the nucleotide dependence of the observed fluorescence changes.

We determined the binding affinity of Dbh for the 2-AP DNA substrates I and II by measuring the rate of primer extension as a function of Dbh concentration (Supporting Information, Figure S1). The apparent K_d values, reflecting the binding constant in the presence of the correct dNTP, were 140 nM for substrate I and 66 nM for substrate II (Table 1). The fluorescence of substrates I and II is at least 2-fold greater when bound to Dbh than when unbound (data not shown), and this provided the means to measure the rate of DNA dissociation from the binary complex. A solution of Dbh bound to the fluorescent DNA substrate I or II was mixed with a solution containing a 20-fold excess of nonfluorescent DNA, and the resulting fluorescence decrease was observed in the stopped-flow instrument (Figure 2), giving dissociation (k_{off}) rates of 150 s^{-1} for substrate I and 130 s^{-1} for substrate II (Table 1).

2-AP at 0 Position with a Correct dTTP. Kinetic analyses of the fluorescent changes accompanying nucleotide binding and addition to DNA substrate I, terminated with a 3′OH, revealed 4 fluorescence transitions (Figure 3A and Table 1). We have assigned the fluorescently detected changes as steps F1, F2, F3, etc. to distinguish them from the kinetically assigned steps 1, 2, 3, etc. of the mechanism in Scheme 1. An initial very rapid fluorescence decrease (step F1) was observed within the instrument dead-time, corresponding to a rate of $\geq$1000 s^{-1}. The amplitude of step F1 was estimated for each dTTP concentration by comparing the fluorescence immediately following the instrument dead-time (~2 ms after mixing) with the fluorescence at the same time point on the control trace in which the binary complex was mixed with reaction buffer alone (Figure 3A). The amplitude had a hyperbolic dependence on nucleotide concentration, similar to the nucleotide concentration dependence of the rate of dTTP addition in chemical quench measurements (Figure 3B and Table 1). Thus, the amplitude indicates the fraction of Dbh−DNA converted to ternary complex at each dTTP concentration, and the fluorescence change F1 results from the initial binding of dNTP to the binary complex or an extremely rapid transition consequent on that initial binding event. Following the fluorescence decrease of step F1 were 2 low amplitude fluorescence changes (see Supporting Information, Figure S2); a decrease at ~100 s^{-1} (step F2) was followed by a fluorescence increase at ~30 s^{-1} (step F3). Steps F2 and F3 were difficult to quantitate accurately, especially at lower dTTP concentrations, and therefore we did not evaluate their nucleotide concentration dependence.

The final fluorescence change observed with substrate I was a decrease (step F4) whose rate was close to the rate of dTTP incorporation measured by chemical quench, suggesting that they may report on the same process (Figure 3C

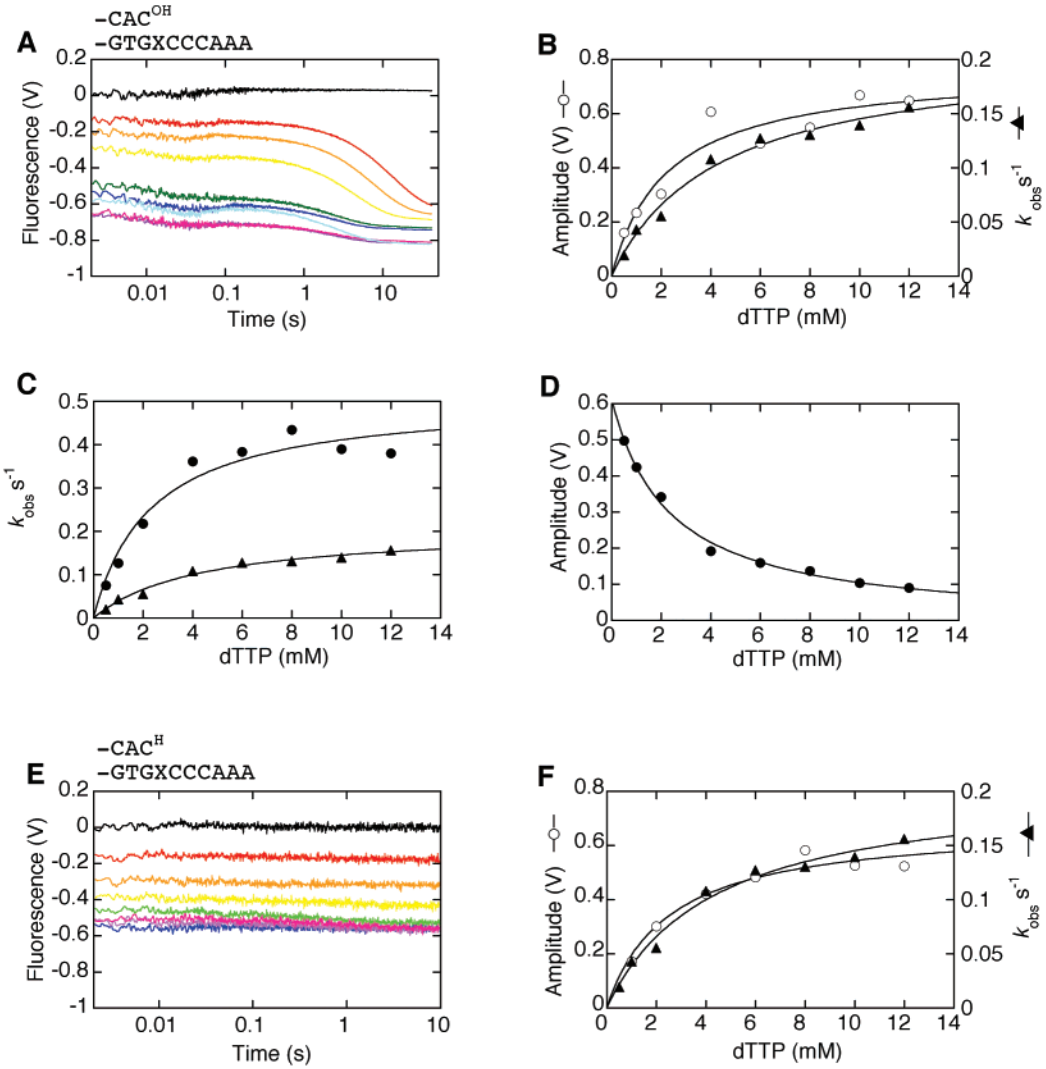

FIGURE 3: 2-AP at the templating (0) position. (A) Stopped-flow kinetics were carried out as described in Experimental Procedures, using a 3'OH-terminated primer. Final dTTP concentrations (mM) in the reaction were 0.5 (red), 1 (orange), 2 (yellow), 4 (pale blue), 6 (green), 8 (dark blue), 10 (purple), 12 (magenta). The black trace was a control in which the second syringe contained reaction buffer without dTTP. The data were plotted using a logarithmic time scale so as to show the early fluorescence changes, which were most pronounced at higher dTTP concentrations (see Supporting Information, Figure S2 for an expanded view of 2 of these traces). (B) dTTP concentration dependence of the amplitude of the fluorescence change that takes place within the instrument dead-time in panel A (step F1), and the rate of nucleotide addition, determined by chemical quench (see Supporting Information, Figure S3 for rate plots). The fluorescence and chemical quench data were fitted to hyperbolae, giving K_d values of 2.2 mM and 4.3 mM, respectively. The corresponding K_d values listed in Table 1 are the averages from at least 2 determinations. (C) Comparison of the rate of dTTP incorporation determined by chemical quench with the rate of the final fluorescence decrease (step F4) shown in panel A. Fitting of the data to hyperbolic equations gave $k_{max} = 0.51$ s^{-1} and $K_{d\ app} = 2.3$ mM for the fluorescence data (filled circles), and $k_{pol} = 0.21$ s^{-1} and $K_d = 4.3$ mM for the chemical quench data (filled triangles). (D) The amplitude of step F4 from panel A as a function of dTTP concentration. As explained in the text, the data fitted a decreasing hyperbola, giving $K_{d\ app} = 2.3$ mM, and approached a minimum amplitude of <0.1 V at high dTTP concentrations. (E) Stopped-flow kinetics with a dideoxy-terminated primer. Final dTTP concentrations (mM) in the reaction were 1 (red), 2 (orange), 4 (yellow), 6 (green), 8 (blue), 10 (purple), 12 (magenta). The black trace was a control in which the second syringe contained reaction buffer without dTTP. (F) dTTP concentration dependence of the amplitude of the fluorescence change that takes place within the instrument dead-time in panel E (step F1), and the rate of nucleotide addition, determined by chemical quench. The fluorescence and chemical quench data were fitted to hyperbolae, giving K_d values of 2.5 mM and 4.3 mM, respectively.

and Table 1). If the F4 fluorescence decrease and the chemical quench rate were reporting on distinct steps within the reaction pathway, we would expect the slower (chemical quench) reaction to show a lag in product formation that is equal to the reciprocal of the rate for the faster (F4) reaction (*47*). On examining the early part of the chemical quench reaction at 2 mM dTTP (data not shown), we did not detect a lag of the expected magnitude (5 s), and we therefore conclude that the fluorescence signal from step F4 and the chemical quench reaction are most probably rate-limited by the same process. The amplitude of step F4 decreased with increasing dTTP concentration; at low dTTP concentrations the amplitude of step F4 was ~0.5 V, but, as the dTTP binding reached saturation, the amplitude decreased to <0.1 V (Figure 3D). At low dTTP concentrations, the initial binding event does not convert 100% of the Dbh−DNA binary complex to the ternary complex and therefore the amplitude of step F4 has an additional contribution from dNTP binding and conversion of binary to ternary complex. However, at high dTTP concentrations, essentially all the Dbh−DNA binary complex is converted to ternary complex within the instrument dead-time, and the amplitude of F4

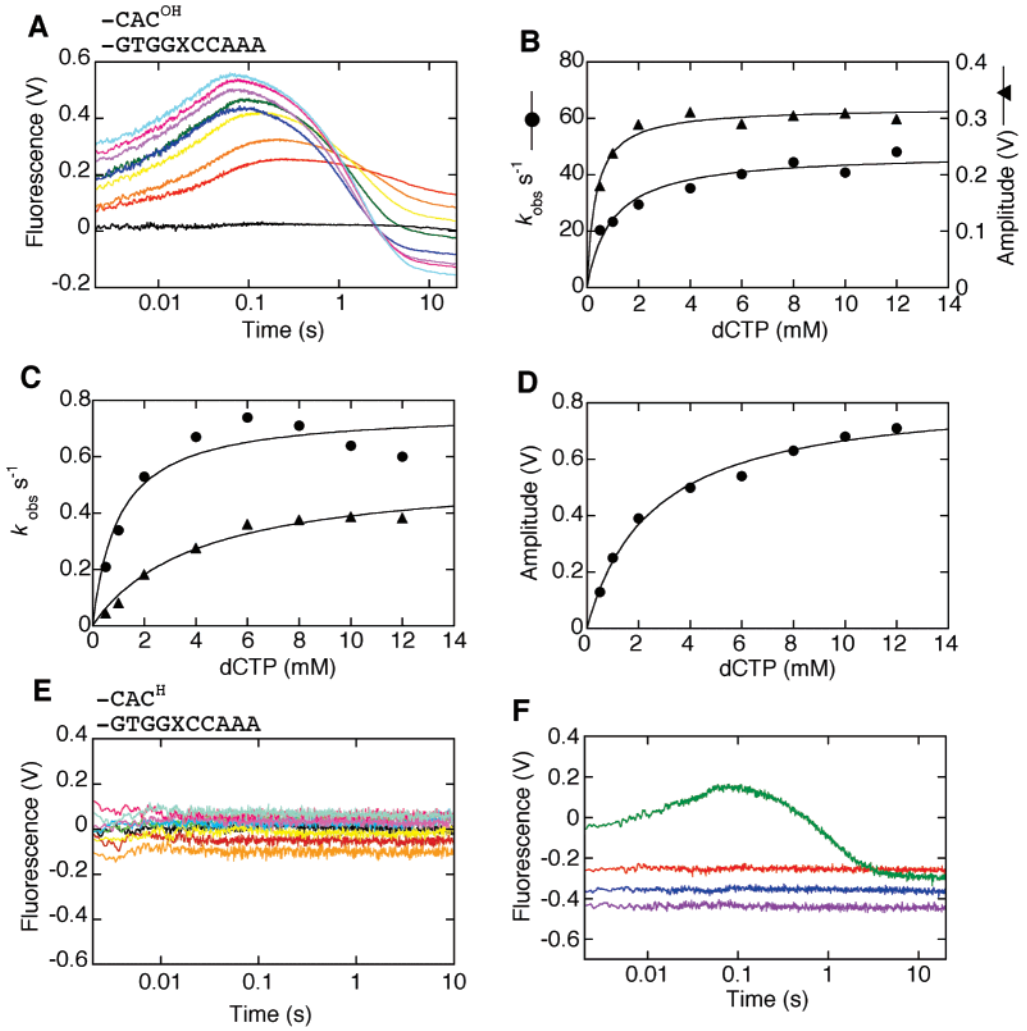

FIGURE 4: 2-AP at the +1 position. (A) Stopped-flow kinetics were carried out as described in Experimental Procedures, using a 3'OH-terminated primer. Final dCTP concentrations (mM) in the reaction were 0.5 (red), 1 (orange), 2 (yellow), 4 (green), 6 (dark blue), 8 (purple), 10 (magenta), 12 (pale blue). The black trace was a control in which the second syringe contained reaction buffer without dCTP. The data were plotted using a logarithmic time scale so as to show the early fluorescence increase (step F1') which was detectable only at low dCTP concentrations. (B) dCTP concentration dependence of the amplitude and rate of the large prechemistry fluorescence increase (step F3) from panel A. Hyperbolic curve fits gave maximum values of 0.3 V (amplitude) and 48 s^{-1} (rate) and a reasonable agreement between the corresponding $K_{d\,app}$ values of 0.34 mM and 0.98 mM. The values listed in Table 1 are the averages from at least 2 determinations. (C) Comparison of the rate of dCTP incorporation determined by chemical quench (see Supporting Information, Figure S3 for rate plots) with the rate of the final fluorescence decrease (step F4) from panel A. Fitting of the data to hyperbolic equations gave $k_{max} = 0.76\ s^{-1}$ and $K_{d\,app} = 1.0$ mM for the fluorescence data (filled circles), and $k_{pol} = 0.55\ s^{-1}$ and $K_d = 4.0$ mM for the chemical quench data (filled triangles). (D) The amplitude of step F4 from panel A as a function of dCTP concentration. The data were fitted to a hyperbola, giving a maximum amplitude of 0.83 V and $K_{d\,app}$ of 2.5 mM. (E) Stopped-flow kinetics with a dideoxy-terminated primer. Final dCTP concentrations (mM) in the reaction were 0.5 (red), 1 (orange), 2 (yellow), 4 (green), 6 (dark blue), 8 (purple), 10 (magenta), 12 (pale blue). The black trace was a control in which the second syringe contained reaction buffer without dCTP. (F) Stopped-flow kinetics for incorrect nucleotide incorporation with an extendable primer at 6 mM dATP (red), dGTP (blue), or dTTP (purple) and the correct nucleotide dCTP (green).

results solely from fluorescence changes later in the reaction pathway. Consistent with this interpretation, the dTTP concentration dependence of the F4 amplitude was the inverse of the concentration dependence of the F1 amplitude, a decreasing hyperbola whose halfway point gave a $K_{d\,app}$ of 1.8 mM, similar to the K_d values derived from F1 and from the chemical quench incorporation rate (Table 1).

In the absence of a 3′OH at the primer terminus, we observed only a rapid fluorescence decrease, presumably the equivalent of step F1, that occurs within the instrument dead-time; none of the subsequent fluorescence changes seen with the 3′OH-terminated primer were observed (Figure 3E). The dTTP concentration dependence of the amplitude for the initial fluorescence quench with the nonextendable primer was similar to that observed with the extendable primer and to the dTTP concentration dependence of the chemical quench experiment (Figure 3F).

The maximum amplitudes of the fluorescence changes occurring within the instrument dead-time (step F1) were ~0.6 V, and we believe that they are a valid reflection of a process within the reaction pathway based on the following controls. Duplicate measurements at the start and finish of a stopped-flow experiment indicated that the amount of drift in the lamp intensity or other instrument parameters was ≤0.2 V. Moreover, we eliminated systematic errors caused by lamp intensity drift by randomizing the sequence of dTTP solutions used in measuring the concentration dependence of fluorescence changes, rather than using the dTTP solutions in ascending or descending order of concentration. We were concerned that the initial fluorescence decrease might be

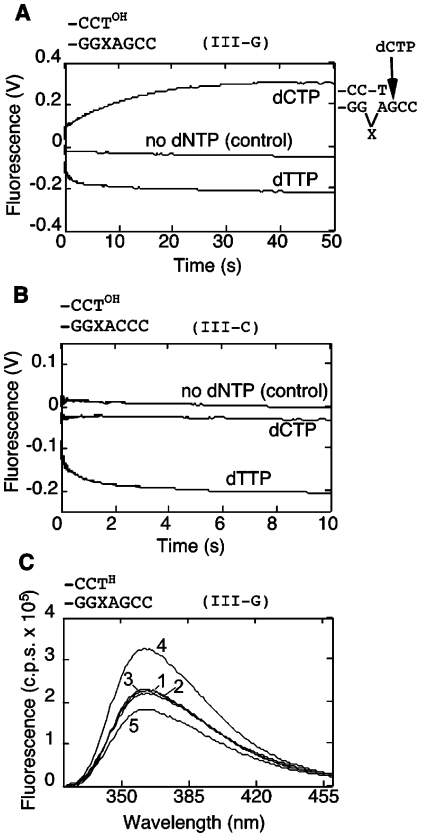

FIGURE 5: Base-skipping reaction observed using 2-AP fluorescence. (A) Fluorescence changes observed in the stopped-flow instrument with final concentrations of 2 mM dCTP (base-skipping) or 2 mM dTTP (correct insertion) added to a binary complex of Dbh with substrate III-G. The control trace corresponds to the addition of reaction buffer without nucleotide. (B) Stopped-flow fluorescence, as in A, using the control substrate III-C with final concentrations of 2 mM dCTP (misinsertion) or 2 mM dTTP (correct insertion). The sequence around the primer terminus of each DNA substrate is shown above the relevant panel, and our interpretation of the arrangement of the template strand during the base-skipping reaction is diagrammed adjacent to panel A. Table 2 lists the rates for the fluorescence changes and chemical quench nucleotide additions to substrates III-G and III-C. (C) Fluorescence emission spectra showing the effect of dNTP addition to a complex of Dbh bound to dideoxy-terminated substrate III-G. Before dNTP addition, the emission spectrum of the binary complex was recorded (trace 1). Traces 2−5 correspond to addition of the following dNTPs (to 4 mM final concentration): 2, dGTP (incorrect); 3, dATP (incorrect); 4, dCTP (complementary to +1 base); 5, dTTP (complementary to 0 base).

caused by an inner-filter effect because of the high concentrations of nucleotide used in our experiments. However, the absorbance of our most concentrated dTTP solution (12 mM) at the 2-AP excitation wavelength (313 nm) was 2.6×10^{-3}, which is too low to cause an inner-filter effect (*48*).

To evaluate the extent of other quenching effects contributed by the high concentrations of nucleotide, we monitored the fluorescence changes that occur within the instrument dead-time when the binary complex was mixed with high concentrations of dTMP (8 or 12 mM) or with any of the 3 incorrect nucleotides (12 mM dNTP/Mg^{2+}). The rationale of this experiment was to use nucleotides that were unlikely to bind the binary complex in a specific manner. On addition of either dTMP (without added Mg^{2+}) or an incorrect nucleotide, there was very little change in fluorescence relative to a control consisting of the binary complex mixed with reaction buffer alone (data not shown).[2] Therefore, the data suggest that the signal for step F1 results from a dTTP/Mg^{2+} dependent change that is "on pathway".

2-AP at +1 Position with a Correct dCTP. Kinetic studies of dCTP addition to the 2-AP(+1) DNA substrate II, terminated with a 3′OH, revealed at least 3 fluorescence transitions of which the last 2 are most probably equivalent to steps F3 and F4 that were observed with 2-AP at the 0 position (Figure 4A and Table 1). Preceding these steps is a very rapid fluorescence increase, much of which takes place within the instrument dead-time. At low dCTP concentrations this early process was seen as an increase, with a rate of $\sim$500 s^{-1}, preceding a larger fluorescence increase, step F3, which has a rate of $\sim$40 s^{-1} (see Supporting Information, Figure S4). At dCTP concentrations above 6 mM the early fluorescence increase is so rapid that it is complete within the instrument dead-time (see Supporting Information, Figure S5). Although it is difficult to determine with confidence the rate and amplitude of this early step, it appears to be intermediate in rate between the F1 and F2 transitions observed with the 0 position 2-AP probe, and we have assigned it as step F1′. It is followed by a step that appears to be equivalent to F3, whose rate and amplitude have the expected hyperbolic dependence on dCTP concentration (Figure 4B).

The prechemistry fluorescence increases of steps F1′ and F3 are followed by a large amplitude fluorescence decrease (F4). The dCTP concentration dependence of the rate of step F4 yielded kinetic parameters similar to those determined by chemical quench for dCTP incorporation (Figure 4C); the amplitude of this step increased with increasing concentrations of dCTP and fit to a hyperbola (Figure 4D). As with the experiments using substrate I, we inferred that the fluorescence decrease and the chemical-quench reaction are probably rate-limited by the same step based on the absence of a lag in product formation in the chemical quench reaction measured at 2 mM dCTP (data not shown). The endpoint of the F4 fluorescence change is influenced by dCTP concentration, being lowest at the highest nucleotide concentrations (Figure 4A). We believe that this results from binding of dCTP opposite 2-AP subsequent to the first dCTP incorporation (see Discussion).

The fluorescence changes described above were observed only when the primer contained a 3′OH and with addition of the correct nucleotide. No fluorescence changes were observed on dCTP addition when the primer was dideoxy-terminated (Figure 4E), providing additional evidence that step F1′ is distinct from step F1. Moreover, with an extendable primer, the fluorescence changes described above were absent on addition of any of the 3 incorrect nucleotides, dATP, dGTP or dTTP (Figure 4F).

Base-Skipping Reaction. Dbh makes single-base deletion errors at a high frequency (up to 40%) when the template strand contains a dinucleotide pyrimidine repeat immediately 3′ to a G (3′-XXG-5′, where one of the pyrimidines, X, is skipped over during DNA synthesis, resulting in a single-

[2] For addition of Mg^{2+} alone, the fluorescence change relative to the buffer control was about half of that observed when the same final concentration of dTTP/Mg^{2+} was added. However, the fluorescence decrease seen on addition of Mg^{2+} alone substantially overestimates the quenching that results from the same concentration of nucleotide-bound Mg^{2+} (as shown by our data with incorrect dNTP/Mg^{2+}).

Table 1: Kinetic Parameters for DNA Substrates I and II Determined by Stopped-Flow Fluorescence and Chemical Quench[a]

	I 2-AP (0), 3′OH	II[b] 2-AP (+1), 3′OH	I 2-AP (0), 3′H
Step F1		**Step F1′**	
k_{max} (s^{-1})	≥1000	≥500	≥1000
amplitude$_{max}$ (V)	0.56 ± 0.2	∼(−0.3)	0.57 ± 0.3
$K_{d\ app}$ (mM)	2.5 ± 0.4		3.7 ± 1.0
Step F2			
k_{max} (s^{-1})	∼100		
amplitude (V)	0.01 − 0.1		
Step F3[c]			
k_{max} (s^{-1})	∼30	41 ± 7	
$K_{d\ app}$ (mM) (from rate)		0.79 ± 0.2	
amplitude (V)	−(0.01 to 0.1)	−(0.36 ± 0.05)	
$K_{d\ app}$ (mM) (from amplitude)		0.42 ± 0.07	
Step F4[c]			
k_{max} (s^{-1})	0.39 ± 0.1	0.74 ± 0.04	
$K_{d\ app}$ (mM) (from rate)	2.0 ± 0.4	0.95 ± 0.07	
amplitude (V)	<0.1	0.86 ± 0.02	
$K_{d\ app}$ (mM) (from amplitude)	1.8 ± 0.4	2.4 ± 0.2	
Chemical Quench			
k_{pol} (s^{-1})	0.20 ± 0.01	0.51 ± 0.05	
K_d (mM)	4.0 ± 0.5	4.8 ± 1.1	
DNA Binding			
$K_{d\ app}$ (nM)	140 ± 30	66[d]	
k_{off} (s^{-1})	150 ± 40	130 ± 4	

[a] Fluorescence data were fitted to a triple exponential with substrate I and a double or triple exponential with substrate II. See Supporting Information Figures S2, S3, S4, and S5 for additional information and examples of the curve fitting and residuals of stopped-flow experiments and rate plots from chemical quench reactions. [b] The first fluorescence change with substrate II was intermediate in rate between steps F1 and F2 with substrate I. It is assigned as step F1′. [c] The dNTP dependence of the rates and amplitudes for steps F3 and F4 was fitted to hyperbolic plots, so we report 2 $K_{d\ app}$ values (derived from the rate and amplitude, respectively) for each of these steps. [d] Single determination. All other values are from at least two determinations and are reported as mean ± SD.

Table 2: Kinetic Parameters for the Base-Skipping Reaction

	base-skipping/misinsertion[a]		correct insertion	
	dCTP[b]		dTTP[b]	
DNA	fluorescence (s^{-1})	chemical quench (s^{-1})	fluorescence (s^{-1})	chemical quench[c] (s^{-1})
III-G	$(4.8 \pm 3) \times 10^{-2}$	$(1.9 \pm 0.1) \times 10^{-2}$	0.73 ± 0.2	0.66
III-C		$(1.5 \pm 1.3) \times 10^{-4}$	1.3 ± 0.3	0.98
IV-G	$(2.2 \pm 0.3) \times 10^{-3}$	$(1.9 \pm 0.004) \times 10^{-3}$		
IV-T		$(4.7 \pm 0.4) \times 10^{-4}$		

[a] For each pair of substrates (e.g., III-G and III-C), the rates for the first substrate correspond to the base-skipping reaction, and the rates with the second substrate correspond to the misinsertion reaction that would compete with the base-skipping reaction. [b] Final dNTP/Mg^{2+} concentrations were 2 mM for substrate III and 4 mM for substrate IV. [c] Single determinations. All other values are the average of at least two determinations and are reported as mean ± SD.

base deletion) (*26*). Our earlier demonstration that a purine-containing template, 3′-AAG-5′, could also undergo the base-skipping reaction at a rate similar to that of the pyrimidine-containing hotspot sequence (*26*) set the stage for using 2-AP fluorescence to investigate how the template DNA is accommodated at the Dbh active site during this process.[3] Substrate III-G (Figure 1) was designed with 2-AP at the −1 position rather than the 0 position because, in the latter situation, the base-skipping reaction could not compete with the rapid misinsertion of dCTP opposite 2-AP.

When dCTP is added to a complex of Dbh bound to substrate III-G, the G at the +1 position templates dCTP incorporation. Chemical quench experiments established that the rate of dCTP addition (at 2 mM) to substrate III-G was 0.019 s^{-1} (data not shown) and that this rate corresponded to the base-skipping pathway, based on the requirement for the templating G at the +1 position (Table 2). When the +1 G was replaced by a C in the control substrate III-C, the rate of primer extension was 100-fold lower, corresponding to misincorporation of dCTP opposite A at the normal templating position. In the stopped-flow instrument, the base-skipping reaction with substrate III-G resulted in a large amplitude fluorescence increase whose rate resembled the chemical quench rate (Figure 5A and Table 2). This large fluorescence increase was preceded by at least one rapid low amplitude change, which may be analogous to the rapid low amplitude changes described earlier for the 0 and +1 2-AP substrates. The large fluorescence increase was dependent

[3] The fluorescent pyrimidine analogue pyrrolo-dC was unsuitable for this study because its fluorescence emission was not sufficiently sensitive to the changes in stacking interactions likely to take place during the deletion reaction (our preliminary studies, and M. D. Barkley, personal communication).

on the presence of a G at the +1 position, as shown by its absence when using the control substrate III-C (Figure 5B), and was therefore diagnostic for the base-skipping process.

For both substrates III-G and III-C, incorporation of dTTP opposite A at the normal templating position resulted in a fluorescence decrease whose rate was close to the corresponding chemical quench rate (Figure 5 and Table 2). The fluorescence changes observed for dTTP addition with 2-AP at the −1 position were qualitatively very similar to those described above for 2-AP at the 0 position (Figure 3A) and included rapid low-amplitude fluorescence changes, but the overall fluorescence change was lower, presumably on account of the more stable stacking of 2-AP with the neighboring bases when located at the −1 position.

When the primer strand of substrate III-G was dideoxy-terminated, addition of dCTP in the stopped-flow instrument resulted in a rapid fluorescence increase (data not shown). This increase was dependent on complementarity between the incoming dNTP and the +1 template base (Figure 5C), consistent with formation of the ternary complex corresponding to the base skipping-reaction. As expected, addition of dTTP, which is complementary to the A at the 0 position, resulted in a fluorescence decrease.

Skipping over the templating base in substrate III-G could be accompanied by dislocation of either the 2-AP at the −1 position or the A at the 0 position, and displacement of either base could in principle decrease the base stacking of 2-AP causing the observed fluorescence increase (*44*). To distinguish between the fluorescence signals of an extrahelical[4] 2-AP and a 2-AP whose 5′ neighbor has become extrahelical, we examined the fluorescence emission spectra of a series of model substrates designed to place 2-AP within a variety of DNA environments (Figure 6). The fluorescence emission of 2-AP that lacked a base-pairing partner (Figure 6, trace 5) was about 19-fold greater than when its 5′ neighbor lacked a base-pairing partner (Figure 6, trace 2). Moreover, the fluorescence of 2-AP adjacent to an extrahelical C (Figure 6, trace 2) was lower than the fluorescence of 2-AP at the −1 position (Figure 6, trace 3), a model for the starting substrate for the base-skipping reaction. Thus, if the 5′ neighbor of 2-AP, the A at the 0 position of substrate III-G, were to become extrahelical during the base-skipping reaction, we would expect to observe a decrease in 2-AP fluorescence. The fluorescence increase observed for the base-skipping reaction, on addition of dCTP to substrate III-G, is therefore most probably the result of the 2-AP at the −1 position becoming unpaired while the A at the adjacent (0) position slips back to base pair at the primer terminus.

Further confirmation of the fluorescence signal that results when the neighbor of the 2-AP reporter becomes extrahelical was provided by substrate IV-G, in which the templating base is not part of a repeat (Figure 1). We expect Dbh-catalyzed addition of dCTP to the IV-G substrate to result in dCTP incorporation opposite the G at the +1 position, while the template C at the 0 position is skipped past and becomes extrahelical but cannot isomerize so as to pair with the primer terminus. Chemical quench data for IV-G and the control substrate IV-T, which lacks the +1 G, showed

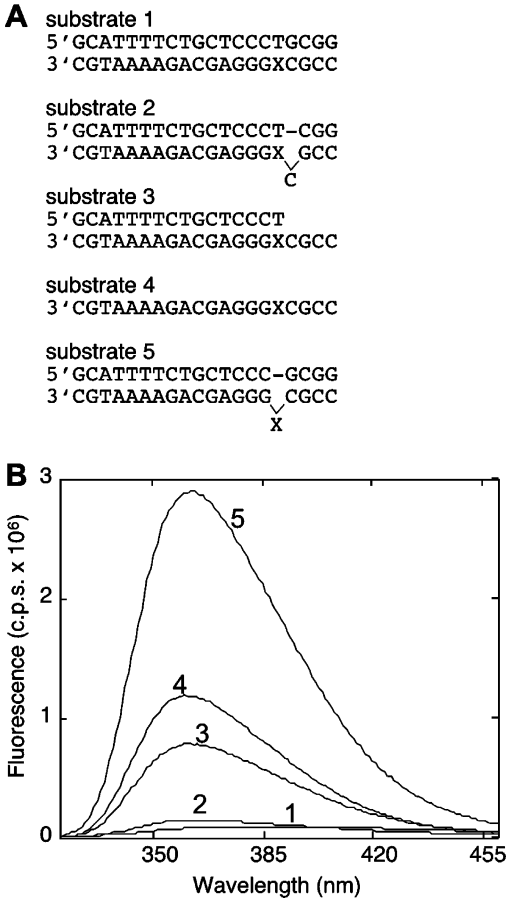

FIGURE 6: Fluorescence emission spectra of model 2-AP substrates. (A) Sequences of model 2-AP-containing DNA substrates, where X indicates 2-AP. (B) Emission spectra of the 2-AP-containing DNAs shown in panel A, using an excitation wavelength of 310 nm. The numbered traces correspond to the DNA sequences listed in panel A: 1, 2-AP in fully duplex DNA; 2, 2-AP whose 5' neighbor lacks a base-pairing partner; 3, a template−primer duplex with 2-AP at the −1 position; 4, 2-AP in single-stranded DNA; 5, 2-AP that lacks a base-pairing partner.

that the base-skipping pathway was preferred by about 4-fold over misinsertion (Table 2). The base-skipping reaction with IV-G was 10-fold slower than with III-G, demonstrating the effect of the dinucleotide repeat in III-G, and it was therefore necessary to monitor the fluorescence signal from substrate IV-G over 1 h (using a fluorometer in time-based mode). On addition of dCTP (to 4 mM) to the binary complex, we observed only a very low amplitude decrease at a rate essentially identical to that of the corresponding chemical quench reaction (Table 2 and Supporting Information, Figure S6). The absence of a fluorescence increase with substrate IV-G confirms the result from the model oligonucleotide experiments, where an extrahelical base adjacent to 2-AP also did not result in a fluorescence increase.

DISCUSSION

Dbh Reaction Pathway. We have investigated the sequence of events following addition of a correctly paired dNTP to a Dbh−DNA binary complex, using 2-AP as a fluorescent reporter. The 2-AP probes respond differently, depending on whether they are located at the 0 or the +1 position on the template strand, presumably reflecting distinct changes in the environment of these bases at each step of the reaction. The 0-position probe reported 3 noncovalent transitions

[4] For brevity, we use the term "extrahelical" to describe the location of a base that lacks a base-pairing partner although, strictly speaking, the location of the base is not known.

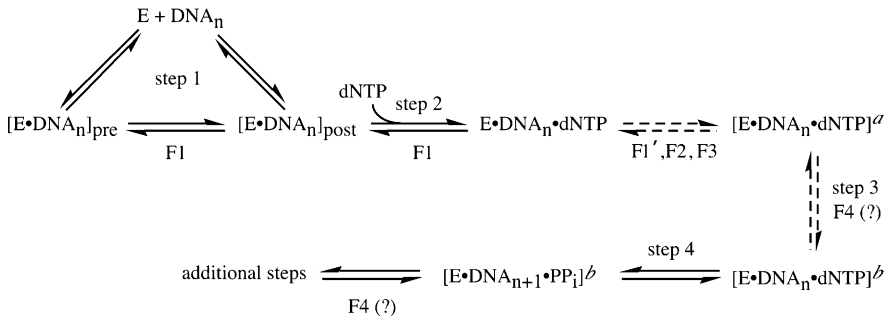

FIGURE 7: Proposed reaction pathway for Dbh. Our fluorescently detected steps (F1, F2, etc.) are placed within the context of the minimal DNA polymerase reaction pathway (steps 1, 2, etc.) from Scheme 1. For a detailed rationale of the placement of the fluorescence transitions within the pathway, see the text. E is Dbh, DNA_n is the DNA primer/template and $[E{\cdot}DNA_n]_{pre}$ and $[E{\cdot}DNA_n]_{post}$ represent the Dbh−DNA binary complex pre- or post-translocation, respectively. The superscripts *a* and *b* designate conformationally distinct forms of the E·DNA·dNTP ternary complex. Dotted arrows indicate areas of uncertainty, the first being a sequence of several noncovalent steps and the second a hypothetical rate-limiting step 3. Because the F4 fluorescence change has the same rate as the rate-limiting step for dNTP incorporation (either step 3 or step 4), its fluorescence signal is the sum of any fluorescence signal from the rate-limiting step and all subsequent rapid fluorescently detectable steps.

before the chemical step. The first (F1), a fluorescence decrease associated with dNTP binding itself or a rapid transition following dNTP binding, is complete within the dead-time of the stopped-flow instrument. It occurs with both extendable and nonextendable (dideoxy-terminated) primers and is the only fluorescence change detected with a nonextendable primer. The absence of a similar fluorescence change with a dideoxy primer when the fluorophore is at the +1 position indicates that the F1 step is fluorescently silent for the +1 probe. Instead, the +1 2-AP shows a fluorescence transition, which we have called F1′, that is almost as fast as F1, being completed within the dead-time at high dNTP concentrations but partially observable at lower concentrations. As far as one can judge from these rapid fluorescence changes, steps F1′ (detectable primarily, or exclusively, with 2-AP at the +1 template base) and F2 (detectable primarily, or exclusively, with 2-AP at the 0 position) are distinct. Step F3, on the other hand, appears to be detected by both reporters, with the larger signal coming from the +1 position. Thus, our current working model is that there are four fluorescence transitions (F1, F1′, F2, and F3, Table 1) that precede the chemical step of dNTP incorporation.

In Figure 7 we have modified the early steps of the minimal DNA polymerase reaction pathway of Scheme 1 so as to incorporate the fluorescence transitions we have detected. This requires the insertion of at least 3 rapid steps (F1′, F2, and F3) between dNTP binding and the rate-limiting step for dNTP incorporation. These prechemistry steps probably represent processes that prepare the active site for phosphoryl transfer by alignment of the metal ions, catalytic residues, and substrates involved in the chemical step. We have also expanded the DNA binding step of the minimal mechanism to include an equilibrium between pre- and post-translocated species that is inferred from the structure of a Dpo4 preinsertion binary complex (2AU0), in which the DNA primer terminus occupies the active site, blocking entry of the incoming dNTP (*15*). If this complex represents the normal position of the primer terminus in binary complexes of Y-family or DinB polymerases in solution, then delivery of the templating base to the active site would require a DNA translocation step. Step 1 of Figure 7 suggests a mechanism for achieving this. Initially the Dbh−DNA binary complex is an equilibrium mixture of pre- and post-translocation species, with the majority as the $E{\cdot}DNA_{pre}$ complex on account of its greater number of protein−DNA contacts. On addition of the correct dNTP, the equilibrium is displaced in favor of the post-translocation configuration as a result of dNTP binding (step 2) to the $E{\cdot}DNA_{post}$ binary complex with an available active site. In this scenario, the F1 fluorescence quench, associated with dNTP binding, would also report on movement of the DNA from the $E{\cdot}DNA_{pre}$ to the $E{\cdot}DNA_{post}$ configuration. Because translocation of the primer terminus causes a substantial change in the environment of the templating base, it could account for much of the large F1 fluorescence decrease.

The final fluorescence change, F4, is a decrease whose rate is the same as the rate-limiting step for dNTP incorporation. The size of the signal is therefore the sum of any fluorescence changes associated with the rate-limiting step and rapid following steps. Indeed, the small F4 decrease reported by the 0 probe and the much larger F4 decrease reported by the +1 probe need not necessarily originate from the same step(s) of the reaction.[5] We have included the rate-limiting noncovalent change, step 3, that precedes phosphoryl transfer because there is good evidence for this step in the Y-family polymerases Dpo4 and yeast DNA pol η (*31*, *32*). For Dbh, however, it is unclear whether this step exists because elemental effect measurements raise the possibility that phosphoryl transfer could be at least partially rate-limiting in correct dNTP addition (*26*, *28*). Therefore contributions to the F4 signal may come from step 3 (if rate-limiting) and from steps following chemistry, whereas phosphoryl transfer itself seems less likely to cause a substantial change in the environment of either of our 2-AP reporter positions.

Our kinetic data and those from another study (*28*) reveal substantial differences in the DNA binding properties of Dbh and its close homologue Dpo4. The DNA binding affinity of Dbh is ~10-fold weaker than that of Dpo4, and the rates for DNA binding and dissociation are ≈1000-fold faster for Dbh than for Dpo4 (*32*). These differences, which are

[5] With substrate II, in which 2-AP is at the +1 position, dCTP incorporation opposite the templating G is followed by translocation and binding of dCTP opposite the new templating base, 2-AP. This accounts for the extremely large F4 fluorescence decrease seen with this 2-AP probe and the dependence of the reaction endpoint on dCTP concentration.

consistent with the lower processivity of Dbh, are probably attributable to differences in the little-finger domains and the associated linker regions of these two closely related polymerases (*14*).

Structural Interpretation. There are several Dpo4 cocrystal structures that may correspond to steps along the kinetic pathway and can therefore provide a context within which to interpret the physical basis of the early fluorescence changes observed in our stopped-flow experiments. The structures (2ASL[6] and 2ATL) solved by Rechkoblit et al. are an appropriately matched pair of binary and ternary complexes of Dpo4 for comparing the positions of the 0 and +1 bases (*15*). In the binary complex (Figure 8A), the 0 base (red) is not stacked with any protein side chains or adjacent template bases, and the +1 base (dark green) is stacked with the +2 base (pale green). Ternary complex formation, and the associated translocation of the primer terminus, results in the 0 base stacking with the primer-terminal base pair and hydrogen bonding to the incoming dCTP, while the +1 base has no stacking interactions (Figure 8B). Movement of the templating base to a more stacked environment on dNTP binding is consistent with the early fluorescence quench (step F1) seen with the 0 position 2-AP reporter. Moreover, the prechemistry fluorescence increases (step F1′ and F3) we observed with the +1 position 2-AP reporter are consistent with the transition of the +1 base to a less stacked environment in the ternary complex. If these assignments are correct, it implies that the movements of these 2 template bases are sequential, not concerted. The substantial differences in the interactions made by the 0 and +1 template bases are consistent with the lack of correlation in their fluorescence signals for individual steps of the reaction. By contrast, the fluorescence transitions of a 2-AP probe at the −1 position parallel those seen with 2-AP at the 0 position, suggesting that the signals from the 0 and −1 positions may report primarily on the mutual stacking of these 2 bases.

Comparison with Other Polymerase Families. Despite the many differences between the Y-family and other DNA polymerase families, the fluorescence changes we have observed with Dbh are remarkably similar to those observed with other DNA polymerase families. Using a 3′OH-terminated DNA substrate having 2-AP at the 0 position, our results with Dbh parallel those previously described for Pol I (KF), T4 DNA pol, and pol β. In all cases, there was an initial rapid fluorescence decrease and a large amplitude fluorescence change that is rate-limited by chemical incorporation, which presumably correspond to steps F1 and F4 respectively (*36*, *39*, *41*, *42*). Steps F2 and F3, observed with Dbh, resemble the low amplitude fluorescence changes that precede the rate-limiting step in the Pol I (KF) reaction (*39*), but were more easily characterized in the present study because of the slower reaction rate of Dbh.

The dNTP-dependent fluorescence decrease (step F1) that takes place within the instrument dead-time with Dbh and a dideoxy-terminated primer having 2-AP at the 0 position is similar to that seen in analogous experiments with Pol I (KF) and T4 DNA pol (*36*, *39*). Therefore, in all cases it appears that formation of the correct ternary complex results in shifting the templating base to a more stacked conformation. The conclusion that a Dbh−DNA−dNTP ternary complex is formed with a dideoxy-terminated primer is consistent with the presence of an incoming nucleotide in Dpo4 ternary complex structures which contain dideoxy-terminated DNA (*2*, *10*, *15*).

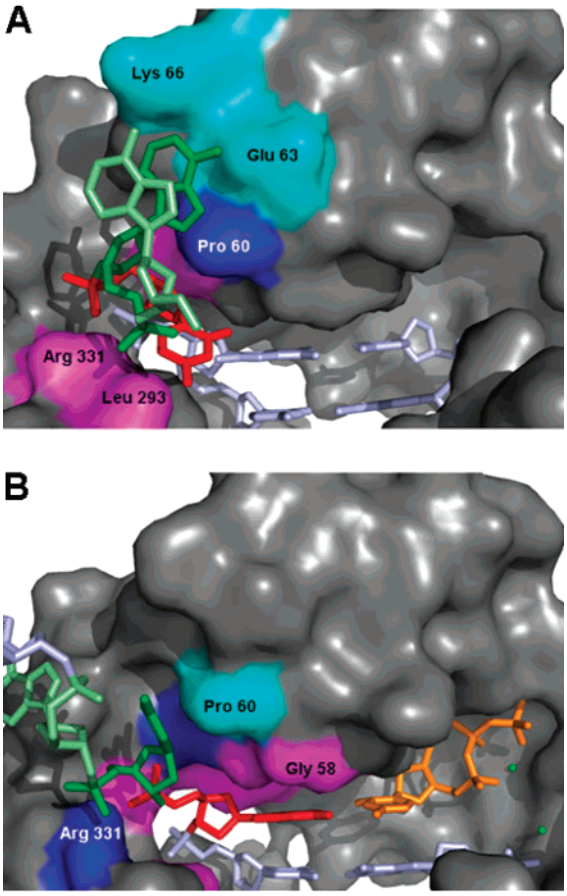

FIGURE 8: Comparison of the positions of the 0 and +1 template bases in binary and ternary Dpo4 complexes. The Dpo4 protein is shown as a gray surface, the duplex DNA, including the primer terminus, is shown in light blue, and the 0, +1, and +2 nucleotides are shown in red, green, and light green respectively. Protein side chains are colored to indicate proximity to the 0 and +1 nucleotides; those within 4 Å of the 0 nucleotide are magenta; those within 4 Å of the +1 nucleotide are cyan; those within 4 Å of both nucleotides are dark blue. (A) Dpo4 postinsertion binary complex (PDB entry 2ASL, ref *15*). The templating (0) base is not stacked with the primer terminus, and protein side chains Gly41, Pro60, Leu293, and Arg331 are within 4 Å of the 0 nucleotide. The +1 base is stacked with the +2 base (light green), and protein side chains Pro60, Glu63, and Lys66 are within 4 Å of the +1 nucleotide. (B) Dpo4 ternary complex (PDB entry 2ATL, ref *15*). The templating (0) base is stacked with the primer terminus and paired opposite the incoming dCTP (orange). Ca^{2+} ions are shown as green spheres. Protein side chains within 4 Å of the 0 nucleotide are Val32, Ser34, Gly41, Ala42, Ala44, Gly58, Arg331, and Arg332. The +1 base is rotated out from the helical axis and is not stacked with protein side chains or adjacent template bases. Gly41, Pro60, and Arg331 are within 4 Å of the +1 nucleotide. Both PDB files have 2 molecules in the asymmetric unit; in each case the positions of the 0 and +1 bases are very similar for both molecules, but there are some minor differences in the side chain interactions. This figure was generated with PyMOL (DeLano Scientific).

[6] Both Dpo4 binary complexes 2AU0 (preinsertion) and 2ASL (postinsertion) represent a pre-translocated configuration; we use the 2ASL complex in our structural interpretation because it provides information on the positions of the nucleotides of the unpaired template strand.

A rapid, prechemistry fluorescence increase has been observed for several DNA polymerases when the 2-AP reporter is at the +1 position, and may therefore represent a common step in the reaction pathway. The F3 transition observed with Dbh resembles changes observed with Pol I (KF) (A-family) and pol β (X-family) (*39*, *40*). T4 and RB69 DNA pols (B-family) show a similar fluorescence increase with 2-AP at the +1 position, but it is unclear whether this increase occurs before chemistry because its rate is very similar to the chemical quench rate and there is no subsequent fluorescence decrease (*37*, *38*, *49*). The structural correlations are also preserved, in that ternary complexes from DNA polymerase families A, B, X, and Y all show a dislocation of the +1 template base from the helical axis (*2*, *16*, *17*, *20*), supporting the idea that the increased fluorescence of the +1 reporter is a consequence of its unstacked conformation in the ternary complex.

The most notable difference between Dbh and other DNA polymerases, such as Pol I (KF) and pol β, concerns the effect of dideoxy-terminated DNA substrates. In Dbh, the 0 position 2-AP reporter indicates that dNTP binding takes place but, unlike Pol I (KF) and pol β (*39*, *40*), no prechemistry fluorescence increase was observed with the +1 2-AP reporter. This implies that the absence of a 3′OH on the primer prevents subsequent steps on the pathway to the formation of an active catalytic center. The primer 3′OH is important because it is located at the heart of the catalytic center and makes contact with the catalytic metal at the A site. Why is the missing 3′OH more detrimental in some polymerases than others? High-fidelity polymerases such as Pol I (KF) and pol β organize their active sites for phosphoryl transfer by creating a snug binding pocket that complements the geometry of the nascent base pair and also provides side chain contacts with the important components of the chemical reaction. Thus, the appropriate geometry can be achieved even in the absence of some key contacts. By contrast, the less constrained binding pocket in bypass polymerases may cause the formation of a catalytically competent active site to be exquisitely sensitive to any changes in the natural substrate (*10*). As pointed out by Vaisman et al., the positions of the metal ions in a Dpo4 ternary complex containing a deoxy-terminated primer terminus are compatible with the requirements of the chemical reaction, whereas those in many Dpo4 ternary complexes with dideoxy-terminated primers are not (*10*).

An important generalization that is emerging from fluorescence studies of DNA polymerases is that the pathway for misincorporation is probably distinct from the pathway for correct dNTP incorporation. In fluorescence studies of a variety of DNA polymerases, including the present study of Dbh, the signals obtained with mispaired dNTPs were quite different from those resulting from correct dNTP addition (*21*, *36*, *39*, *40*). For example, mispaired dNTPs abolish the rapid fluorescence increase seen with the 2-AP reporter at the +1 position, suggesting that the misincorporation pathway does not generate the unstacked conformation of the +1 base, discussed above (Figure 4F, and refs *39*, *40*). The fluorescence results are consistent with the idea that DNA polymerases may have alternative reaction pathways, corresponding to correct incorporation and several different subsets of misincorporations, and that the existence of different pathways for correct and incorrect nucleotides may enhance fidelity by providing kinetic checkpoints which serve as opportunities to reject mismatched substrates (*21*, *23*, *50*, *51*). Therefore, while the details of DNA synthesis may differ among polymerase families, it appears that DNA polymerases have a common strategy for discrimination against mispairs by perturbing the normal reaction pathway used in correct DNA synthesis.

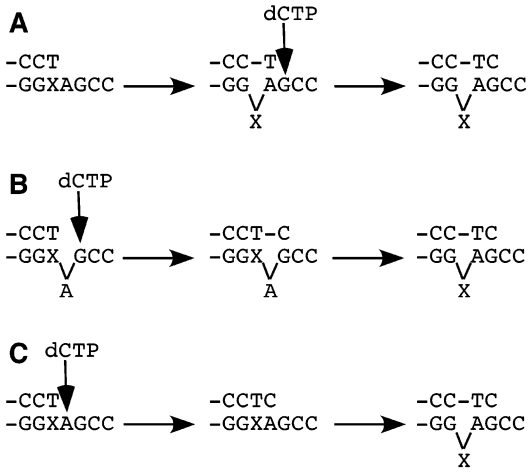

FIGURE 9: Base-skipping pathways that generate unstacking of the base initially paired at the primer terminus. The sequence shown corresponds to substrate III-G, where X is 2-AP. (A) Classical Streisinger slippage mechanism where slippage of the template strand allows the 0 position base, A, to pair at the primer terminus, causing 2-AP to become unpaired. Correct dCTP incorporation opposite the 5' neighbor of the original templating base stabilizes misalignment of the template strand. (B) dNTP-stabilized misalignment of dCTP opposite the +1 base causes the 0 position base, A, to be skipped. Isomerization of the unpaired base from A to the base initially paired with the primer terminus results in unstacking of 2-AP. (C) dCTP misinsertion opposite the templating base, A, is followed by a rearrangement of the template strand which produces 2 correct base pairs at the primer terminus and stabilizes unstacking of 2-AP.

Mechanism of the Base-Skipping Reaction. Our results show that, when Dbh skips a single-base within a dinucleotide run of A and 2-AP (substrate III-G), the base that should have templated the next (normal) addition slips back to pair with the primer terminus while the base previously paired with the primer terminus is pushed out of the base-pairing stack (Figure 5A). The involvement of the terminal base pair is consistent with the effect of run length on the frequency of single-base deletion errors; Dbh deletes single pyrimidines within a dinucleotide run at a 10-fold higher frequency than with a noniterative sequence, and increasing the length of the homopolymeric run beyond a dinucleotide does not substantially increase the deletion frequency (*26*).

Figure 9 shows 3 pathways for base skipping whose end result is unstacking of the template base initially paired at the primer terminus (*52*). Pathway A is a classical Streisinger slippage mechanism in which the primer terminus relocates so as to pair with the 0 position base and subsequent dNTP addition stabilizes the misaligned template. Pathway B is initiated by dNTP incorporation opposite the 5′ neighbor of the normal (0 position) templating base; this first step has been described as "active-site misalignment" or "dNTP-stabilized misalignment" and results in unstacking of the skipped templating base (*53*−*55*). If the dNTP-stabilized misalignment process were followed by an isomerization (second step of pathway B), it could lead to unstacking of

the base originally paired with the primer terminus. Pathway C, in which template misalignment occurs only after misinsertion, can be ruled out for Dbh because the misinsertion rates with our control substrates III-C and IV-T were slower than the base-skipping reactions with the corresponding substrates III-G and IV-G (Table 2).

Because the rate of the fluorescence increase associated with the base-skipping reaction is similar to the rate of dCTP incorporation measured by chemical quench, we conclude that both phosphoryl transfer and the rearrangement that results in unstacking of the 2-AP base are probably rate-limited by the same process. In pathway B, dNTP incorporation or an earlier step would be rate-limiting so that the fluorescence increase, caused by the subsequent rapid isomerization of the template strand, would reflect this same rate. If pathway A is written as a simple sequential mechanism, as in Figure 9, the initiating event appears to be slippage of the primer terminus in response to the presence of the dNTP complementary to the +1 template base. A more plausible reaction pathway would have the binary complex as an equilibrium mixture with a small fraction having a misaligned (Streisinger-like) template. Binding of the dNTP that is complementary to the templating base of the misaligned substrate will displace the equilibrium so that more of the misaligned species will be formed, resulting in a fluorescence increase at the same rate as dNTP addition. The fluorescence increase observed on addition of dCTP to substrate III-G with a dideoxy-terminated primer implies that slippage of the primer terminus could occur prior to covalent addition of dCTP, arguing in favor of pathway A.

Mutational spectra from *E. coli* Pol IV (DinB) and Dpo4 are very similar to that of Dbh, both in the high frequency of single-base deletions and in their sequence specificity (*26*, *45*, *46*). Despite this similarity, and in stark contrast to our results with Dbh, 2-AP fluorescence studies of the Pol IV base-skipping reaction (with 2-AP at the 0 position) have been interpreted as indicating that it occurs via a dNTP-stabilized misalignment mechanism (first step of Figure 9B), where the 0 position base rather than its 3′ neighbor becomes extrahelical (*45*, *56*).[7] Paradoxically, the fluorescence signal observed with Pol IV was found to require a template with a run of more than 2 identical bases. Such a homopolymeric run, a hallmark of the Streisinger slippage process, would not be expected to play a role in dNTP-stabilized misalignment.

There are several ternary complex structures of Dpo4 with misaligned DNA substrates that may represent intermediates or products in the base-skipping pathway (*2*, *9*, *11*, *57*). Some of these structures resemble an intermediate in the dNTP-stabilized misalignment pathway (first step of Figure 9B), where the 0 position base is skipped and its 5′ neighbor templates dNTP addition (*2*, *11*, *57*); however, their distorted active site geometry suggests that they would not be catalytically competent (*10*). By contrast, the Ab-2A complex of Dpo4 has the active-site metal ions in suitable positions for phosphoryl transfer (*9*, *10*). The template strand in this complex has an unpaired abasic site stabilized by a correct base pair at the primer terminus, resembling the template arrangement predicted by our fluorescence data, although it lacks a template base at the unpaired position. Cocrystal complexes have also been obtained of the human X-family DNA polymerase, Pol λ, with DNA duplexes designed to form Streisinger-type deletion intermediates and products. In these structures, the unpaired base is located as illustrated in pathway A (Figure 9), and makes specific interactions with the polymerase (*58*). In the Dbh apoenzyme structure, Silvian et al. have noted a "V-shaped groove" between the fingers and little-finger domain that could similarly accommodate template strand bulges (*6*).

In view of the likely involvement of the little-finger domain in contacts to putative misaligned structures, it is important to note that this domain shows more sequence divergence than the polymerase catalytic core (*7*).[8] Variations within this domain may play an important role in determining lesion bypass specificity throughout the Y-family, and, even within the DinB subgroup, they could result in subtle differences in the interaction with intermediates in the base-skipping pathway.

ACKNOWLEDGMENT

We are grateful to Enrique De La Cruz and Anna M. Pyle for use of their stopped-flow instruments and to Enrique De La Cruz for helpful discussions.

SUPPORTING INFORMATION AVAILABLE

The $K_{d\,app}$ measurement for Dbh binding to substrate I is shown in Figure S1. Examples of curve fitting and residuals for stopped-flow experiments and rate plots from chemical quench measurements with DNA substrates I and II are shown in Figures S2, S3, S4, and S5. Figure S6 shows data on the formation of a single-base deletion product with DNA substrate IV. This material is available free of charge via the Internet at http://pubs.acs.org.

REFERENCES

1. Goodman, M. F. (2002) Error-prone repair DNA polymerases in prokaryotes and eukaryotes, *Annu. Rev. Biochem. 71*, 17−50.
2. Ling, H., Boudsocq, F., Woodgate, R., and Yang, W. (2001) Crystal structure of a Y-family DNA polymerase in action: a mechanism for error-prone and lesion-bypass replication, *Cell 107*, 91−102.
3. Zhou, B.-L., Pata, J. D., and Steitz, T. A. (2001) Crystal structure of a DinB lesion bypass DNA polymerase catalytic fragment reveals a classic polymerase catalytic domain, *Mol. Cell 8*, 427−437.
4. Trincao, J., Johnson, R. E., Escalante, C. R., Prakash, S., Prakash, L., and Aggarwal, A. K. (2001) Structure of the catalytic core of *S. cerevisiae* DNA polymerase η: implications for translesion DNA synthesis, *Mol. Cell 8*, 417−426.
5. Uljon, S. N., Johnson, R. E., Edwards, T. A., Prakash, S., Prakash, L., and Aggarwal, A. K. (2004) Crystal structure of the catalytic core of human DNA polymerase Kappa, *Structure (Cambridge) 12*, 1395−1404.
6. Silvian, L. F., Toth, E. A., Pham, P., Goodman, M. F., and Ellenberger, T. (2001) Crystal structure of a DinB family error-prone DNA polymerase from *Sulfolobus solfataricus*, *Nat. Struct. Biol. 8*, 984−989.
7. Yang, W. (2003) Damage repair DNA polymerases Y, *Curr. Opin. Struct. Biol. 13*, 23−30.

[7] The evidence presented by Tippin et al. (*56*) strongly suggests that the base that becomes extrahelical is determined by the specific base-skipping mechanism of the polymerase, not by the relative energetics of 2-AP-T and A-T base pairs.

[8] For example, the amino acid sequence identity between *E. coli* Pol IV and Dbh is 40% within the catalytic core but only 29% overall, as determined by alignment of their primary amino acid sequences with LALIGN, http://www.ch.embnet.org/software/LALIGN_form.html (A. M. DeLucia, unpublished observations).

8. Ling, H., Boudsocq, F., Plosky, B. S., Woodgate, R., and Yang, W. (2003) Replication of a *cis-syn* thymine dimer at atomic resolution, *Nature 424*, 1083−1087.
9. Ling, H., Boudsocq, F., Woodgate, R., and Yang, W. (2004) Snapshots of replication through an abasic lesion; structural basis for base substitutions and frameshifts, *Mol. Cell 13*, 751−762.
10. Vaisman, A., Ling, H., Woodgate, R., and Yang, W. (2005) Fidelity of Dpo4: effect of metal ions, nucleotide selection and pyrophosphorolysis, *EMBO J. 24*, 2957−2967.
11. Zang, H., Goodenough, A. K., Choi, J. Y., Irimia, A., Loukachevitch, L. V., Kozekov, I. D., Angel, K. C., Rizzo, C. J., Egli, M., and Guengerich, F. P. (2005) DNA adduct bypass polymerization by *Sulfolobus solfataricus* DNA polymerase Dpo4: analysis and crystal structures of multiple base pair substitution and frameshift products with the adduct 1, N2-ethenoguanine, *J. Biol. Chem. 280*, 29750−29764.
12. Zang, H., Irimia, A., Choi, J. Y., Angel, K. C., Loukachevitch, L. V., Egli, M., and Guengerich, F. P. (2006) Efficient and high fidelity incorporation of dCTP opposite 7,8-dihydro-8-oxodeoxyguanosine by *Sulfolobus solfataricus* DNA polymerase Dpo4, *J. Biol. Chem. 281*, 2358−2372.
13. Nair, D. T., Johnson, R. E., Prakash, S., Prakash, L., and Aggarwal, A. K. (2004) Replication by human DNA polymerase-ι occurs by Hoogsteen base-pairing, *Nature 430*, 377−380.
14. Boudsocq, F., Kokoska, R. J., Plosky, B. S., Vaisman, A., Ling, H., Kunkel, T. A., Yang, W., and Woodgate, R. (2004) Investigating the role of the little finger domain of Y-family DNA polymerases in low fidelity synthesis and translesion replication, *J. Biol. Chem. 279*, 32932−32940.
15. Rechkoblit, O., Malinina, L., Cheng, Y., Kuryavyi, V., Broyde, S., Geacintov, N. E., and Patel, D. J. (2006) Stepwise translocation of Dpo4 polymerase during error-free bypass of an oxoG lesion, *PLoS Biol. 4*, e11.
16. Doublié, S., Tabor, S., Long, A., Richardson, C. C., and Ellenberger, T. (1998) Crystal structure of a bacteriophage T7 DNA replication complex at 2.2 Å resolution, *Nature 391*, 251−258.
17. Franklin, M. C., Wang, J., and Steitz, T. A. (2001) Structure of the replicating complex of a pol α family DNA polymerase, *Cell 105*, 657−667.
18. Huang, H., Chopra, R., Verdine, G. L., and Harrison, S. C. (1998) Structure of a covalently trapped catalytic complex of HIV-1 reverse transcriptase: implications for drug resistance, *Science 282*, 1669−1675.
19. Li, Y., Korolev, S., and Waksman, G. (1998) Crystal structures of open and closed forms of binary and ternary complexes of *Thermus aquaticus* DNA polymerase I: structural basis for nucleotide incorporation, *EMBO J. 17*, 7514−7525.
20. Sawaya, M. R., Prasad, R., Wilson, S. H., Kraut, J., and Pelletier, H. (1997) Crystal structures of human DNA polymerase β complexed with gapped and nicked DNA: evidence for an induced fit mechanism, *Biochemistry 36*, 11205−11215.
21. Tsai, Y.-C., and Johnson, K. A. (2006) A new paradigm for DNA polymerase specificity, *Biochemistry 45*, 9675−9687.
22. Wong, I., Patel, S. S., and Johnson, K. A. (1991) An induced-fit kinetic mechanism for DNA replication fidelity: direct measurement by single-turnover kinetics, *Biochemistry 30*, 526−537.
23. Joyce, C. M., and Benkovic, S. J. (2004) DNA polymerase fidelity: kinetics, structure, and checkpoints, *Biochemistry 43*, 14317−14324.
24. Kuchta, R. D., Benkovic, P., and Benkovic, S. J. (1988) Kinetic mechanism whereby DNA polymerase I (Klenow) replicates DNA with high fidelity, *Biochemistry 27*, 6716−6725.
25. Johnson, S. J., Taylor, J. S., and Beese, L. S. (2003) Processive DNA synthesis observed in a polymerase crystal suggests a mechanism for the prevention of frameshift mutations, *Proc. Natl. Acad. Sci. U.S.A. 100*, 3895−3900.
26. Potapova, O., Grindley, N. D. F., and Joyce, C. M. (2002) The mutational specificity of the Dbh lesion bypass polymerase and its implications, *J. Biol. Chem. 277*, 28157−28166.
27. DeLucia, A. M., Grindley, N. D. F., and Joyce, C. M. (2003) An error-prone family Y DNA polymerase (DinB homolog from *Sulfolobus solfataricus*) uses a 'steric gate' residue for discrimination against ribonucleotides, *Nucleic Acids Res. 31*, 4129−4137.
28. Cramer, J., and Restle, T. (2005) Pre-steady-state kinetic characterization of the DinB homologue DNA polymerase of *Sulfolobus solfataricus*, *J. Biol. Chem. 280*, 40552−40558.
29. Potapova, O., Chan, C., DeLucia, A. M., Helquist, S. A., Kool, E. T., Grindley, N. D. F., and Joyce, C. M. (2006) DNA polymerase catalysis in the absence of Watson-Crick hydrogen bonds: analysis by single-turnover kinetics, *Biochemistry 45*, 890−898.
30. DeLucia, A. M., Chaudhuri, S., Potapova, O., Grindley, N. D. F., and Joyce, C. M. (2006) The properties of steric gate mutants reveal different constraints within the active sites of Y-family and A-family DNA polymerases, *J. Biol. Chem. 281*, 27286−27291.
31. Washington, M. T., Prakash, L., and Prakash, S. (2001) Yeast DNA polymerase η utilizes an induced-fit mechanism of nucleotide incorporation, *Cell 107*, 917−927.
32. Fiala, K. A., and Suo, Z. (2004) Mechanism of DNA polymerization catalyzed by *Sulfolobus solfataricus* P2 DNA polymerase IV, *Biochemistry 43*, 2116−2125.
33. Patel, S. S., Wong, I., and Johnson, K. A. (1991) Pre-steady-state kinetic analysis of processive DNA replication including complete characterization of an exonuclease-deficient mutant, *Biochemistry 30*, 511−525.
34. Dahlberg, M. E., and Benkovic, S. J. (1991) Kinetic mechanism of DNA polymerase I (Klenow fragment): identification of a second conformational change and evaluation of the internal equilibrium constant, *Biochemistry 30*, 4835−4843.
35. Frey, M. W., Sowers, L. C., Millar, D. P., and Benkovic, S. J. (1995) The nucleotide analog 2-aminopurine as a spectroscopic probe of nucleotide incorporation by the Klenow fragment of *Escherichia coli* polymerase I and bacteriophage T4 DNA polymerase, *Biochemistry 34*, 9185−9192.
36. Fidalgo da Silva, E., Mandal, S. S., and Reha-Krantz, L. J. (2002) Using 2-aminopurine fluorescence to measure incorporation of incorrect nucleotides by wild type and mutant bacteriophage T4 DNA polymerases, *J. Biol. Chem. 277*, 40640−40649.
37. Yang, G., Wang, J., and Konigsberg, W. (2005) Base selectivity is impaired by mutants that perturb hydrogen bonding networks in the RB69 DNA polymerase active site, *Biochemistry 44*, 3338−3346.
38. Mandal, S. S., Fidalgo, da Silva, E., and Reha-Krantz, L. J. (2002) Using 2-aminopurine fluorescence to detect base unstacking in the template strand during nucleotide incorporation by the bacteriophage T4 DNA polymerase, *Biochemistry 41*, 4399−4406.
39. Purohit, V., Grindley, N. D. F., and Joyce, C. M. (2003) Use of 2-aminopurine fluorescence to examine conformational changes during nucleotide incorporation by DNA polymerase I (Klenow fragment), *Biochemistry 42*, 10200−10211.
40. Dunlap, C. A., and Tsai, M.-D. (2002) Use of 2-aminopurine and tryptophan fluorescence as probes in kinetic analyses of DNA polymerase β, *Biochemistry 41*, 11226−11235.
41. Shah, A. M., Li, S.-X., Anderson, K. S., and Sweasy, J. B. (2001) Y265H mutator mutant of DNA polymerase β. Proper geometric alignment is critical for fidelity, *J. Biol. Chem. 276*, 10824−10831.
42. Arndt, J. W., Gong, W., Zhong, X., Showalter, A. K., Liu, J., Dunlap, C. A., Lin, Z., Paxson, C., Tsai, M.-D., and Chan, M. K. (2001) Insight into the catalytic mechanism of DNA polymerase β: structures of intermediate complexes, *Biochemistry 40*, 5368−5375.
43. Sowers, L. C., Fazakerley, G. V., Eritja, R., Kaplan, B. E., and Goodman, M. F. (1986) Base pairing and mutagenesis: observation of a protonated base pair between 2-aminopurine and cytosine in an oligonucleotide by proton NMR, *Proc. Natl. Acad. Sci. U.S.A. 83*, 5434−5438.
44. Rachofsky, E. L., Osman, R., and Ross, J. B. (2001) Probing structure and dynamics of DNA with 2-aminopurine: effects of local environment on fluorescence, *Biochemistry 40*, 946−956.
45. Kobayashi, S., Valentine, M. R., Pham, P., O'Donnell, M., and Goodman, M. F. (2002) Fidelity of *Escherichia coli* DNA polymerase IV. Preferential generation of small deletion mutations by dNTP-stabilized misalignment, *J. Biol. Chem.* ***277***, 34198−34207.
46. Kokoska, R. J., Bebenek, K., Boudsocq, F., Woodgate, R., and Kunkel, T. A. (2002) Low fidelity DNA synthesis by a Y family DNA polymerase due to misalignment in the active site, *J. Biol. Chem. 277*, 19633−19638.
47. Johnson, K. A. (2003) *Kinetic Analysis of Macromolecules*, Oxford University Press.
48. Lakowicz, J. R. (1999) *Principles of Fluorescence Spectroscopy*, 2nd ed., Kluwer Academic/Plenum Publishers, New York.
49. Hariharan, C., Bloom, L. B., Helquist, S. A., Kool, E. T., and Reha-Krantz, L. J. (2006) Dynamics of nucleotide incorporation: snapshots revealed by 2-aminopurine fluorescence studies, *Biochemistry 45*, 2836−2844.

50. Krahn, J. M., Beard, W. A., and Wilson, S. H. (2004) Structural insights into DNA polymerase β deterrents for misincorporation support an induced-fit mechanism for fidelity, *Structure 12*, 1823−1832.
51. Arora, K., Beard, W. A., Wilson, S. H., and Schlick, T. (2005) Mismatch-induced conformational distortions in polymerase β support an induced-fit mechanism for fidelity, *Biochemistry 44*, 13328−13341.
52. Kunkel, T. A., and Bebenek, K. (2000) DNA replication fidelity, *Annu. Rev. Biochem. 69*, 497−529.
53. Kunkel, T. A. (1986) Frameshift mutagenesis by eucaryotic DNA polymerases in vitro, *J. Biol. Chem. 261*, 13581−13587.
54. Efrati, E., Tocco, G., Eritja, R., Wilson, S. H., and Goodman, M. F. (1997) Abasic translesion synthesis by DNA polymerase beta violates the "A-rule". Novel types of nucleotide incorporation by human DNA polymerase β at an abasic lesion in different sequence contexts, *J. Biol. Chem. 272*, 2559−2569.
55. Garcia-Diaz, M., and Kunkel, T. A. (2006) Mechanism of a genetic glissando: structural biology of indel mutations, *Trends Biochem. Sci. 31*, 206−214.
56. Tippin, B., Kobayashi, S., Bertram, J. G., and Goodman, M. F. (2004) To slip or skip, visualizing frameshift mutation dynamics for error-prone DNA polymerases, *J. Biol. Chem. 279*, 45360−45368.
57. Ling, H., Sayer, J. M., Plosky, B. S., Yagi, H., Boudsocq, F., Woodgate, R., Jerina, D. M., and Yang, W. (2004) Crystal structure of a benzo[a]pyrene diol epoxide adduct in a ternary complex with a DNA polymerase, *Proc. Natl. Acad. Sci. U.S.A. 101*, 2265−2269.
58. Garcia-Diaz, M., Bebenek, K., Krahn, J. M., Pedersen, L. C., and Kunkel, T. A. (2006) Structural analysis of strand misalignment during DNA synthesis by a human DNA polymerase, *Cell 124*, 331−342.

BI7006756